# LUND UNIVERSITY

## Quantitative K-Cl-S chemistry in thermochemical conversion processes using in situ optical diagnostics

Weng, Wubin; Li, Zhongshan; Wu, Hao; Aldén, Marcus; Glarborg, Peter

# Quantitative K-Cl-S chemistry in thermochemical conversion processes using in situ optical diagnostics

Wubin Weng [a], Zhongshan Li [a,*], Hao Wu [b], Marcus Aldén [a], Peter Glarborg [b]

[a] *Division of Combustion Physics, Lund University, P.O. Box 118, SE221 00 Lund, Sweden*
[b] *Department of Chemical and Biochemical Engineering, Technical University of Denmark, DK-2800 Kgs. Lyngby, Denmark*

**Abstract**

The sulfation of gas-phase KOH and KCl was investigated in both oxidizing and reducing atmospheres at temperatures of 1120 K, 1260 K, 1390 K, and 1550 K. Well-defined gas environments were generated in a laminar flame burner fuelled with $CH_4$/air/$O_2$/$N_2$. Atomized $K_2CO_3$ and KCl water solution fog and $SO_2$ were introduced into the hot gas as sources of potassium, chlorine, and sulfur, respectively. The in situ concentrations of KOH, KCl, and OH radicals were measured using broadband UV absorption spectroscopy, and the concentration of K atom was measured using TDLAS at 769.9 nm and 404.4 nm. The nucleated and condensed $K_2SO_4$ aerosols were visualized as illuminated by a green laser sheet. With $SO_2$ addition, reduced concentrations of KOH, KCl, and K atom were measured in the hot gas. The sulfation was more significant for the low temperature cases. KOH was sulfated more rapidly than KCl. $K_2SO_4$ aerosols, formed by homogeneous nucleation, were observed at temperatures below 1260 K. At 1390 K, no aerosols were formed, indicating that the consumed KOH was transformed into gaseous $KHSO_4$ or $K_2SO_4$. K atoms formed in the hot flue gas with KOH addition enhanced the consumption of OH radicals except at the high-temperature case at 1550 K. At 1120 K and 1260 K, the sulfation of KOH with $SO_2$ seeding reduced the concentration of K atom, resulting in less OH radical consumption. Studies were also conducted in a hot reducing environment at 1140 K, with the flame at an equivalence ratio of 1.31. Similar to the observation in the oxidizing atmosphere, the concentrations of KOH and K atom decreased dramatically with $SO_2$ seeding. An unknown absorption spectrum observed was attributed to UV absorption by KOSO. The experimental results were used to evaluate a detailed K-Cl-S reaction mechanism, and a reasonable agreement was obtained.

---

* Corresponding author.
*E-mail address:* zhongshan.li@forbrf.lth.se (Z. Li).

## 1. Introduction

Fouling, slagging, and corrosion are severe problems in operating furnaces when utilizing biomass fuels, mostly due to the varying amounts of potassium and chlorine contained in the fuels. The sulfation of KCl to $K_2SO_4$ can be one of the most effective methods to mitigate the negative effect, because $K_2SO_4$ has a higher melting point and is less corrosive than KCl. The sulfation process can be achieved through homogenous reactions between gaseous KCl/ KOH and sulfur oxides. The reactions, especially the sulfation of KCl, have been studied by quite a few researchers [1–14].

Glarborg and Marshall [2] proposed a detail chemical mechanism to describe the sulfation process, and it was evaluated by comparing predictions with the experimental results reported by Iisa et al. [1]. Hindiyarti et al. [5] extended the mechanism by adding a number of alternative sulfation routes. Ekvall et al. [10] used this mechanism to model the sulfation chemistry in oxy-fuel atmospheres. Different experimental studies [6,8,13] have been conducted aiming at the confirmation of the suggested sulfation pathways involved in the chemical mechanism. However, more quantitative experimental results in a well-defined homogenous gas environment are still desired to evaluate the detailed reaction mechanism.

Li et al. [9] studied the sulfation of KCl by $SO_2$ in a homogeneous hot gas environment produced by a laminar flame burner. The concentrations of KCl and HCl in the hot gas were measured using in-situ optical diagnostics, i.e., UV absorption spectroscopy and infrared polarization spectroscopy. However, to obtain a better understanding of the detailed mechanism, additional quantitative results are required, such as the concentrations of other potassium species, i.e., KOH and K atom, and the OH radicals. Therefore, in the present work, the sulfation process of KOH and KCl was further investigated through quantitative measurements of KOH, KCl, K atoms, and OH radicals in different well-defined hot gas environments. A laminar flame burner was adopted to provide hot gas flows at a temperature between 1120 K and 1550 K. Both oxidative and reducing atmospheres were employed. The hot gas environments were close to the operating conditions of fluidized bed gasifiers (about 1100–1300 K) [15]. In this temperature range, the data was still rarely available in the literature. The concentrations of KOH, KCl, and OH were measured using a well-developed UV absorption spectroscopy method [16,17]. The concentration of K atoms was measured using tunable diode laser absorption spectroscopy (TDLAS) at 769.9 nm and 404.4 nm to cover the necessary dynamic range from ppb to ppm level. A detailed reaction mechanism developed by Weng et al. [13] was evaluated through a comparison of the simulation and experimental results.

## 2. Methods

Hot gas environments were generated using laminar flames stabilized on a multi-jet burner (cf. Fig. 1a), which has a rectangular outlet of 85 mm × 47 mm (cf. Fig. 1b), and are described in detail elsewhere [18]. Anchored on the outlets of the 181 jets, a premixed flame matrix was formed as premixed $CH_4/air/O_2$ was introduced into the jet chamber of the burner. Air and $N_2$ were introduced into the co-flow chamber, providing an evenly distributed co-flow surrounding the premixed jet flames. The co-flow gas mixed rapidly into the hot gas production from jet flames, where a homogenous hot flue gas flow was generated above the burner outlet with a selected temperature and oxygen concentration as the reaction environment. As shown in Fig. 1a, the burner outlet is ~29 mm above the premixed flame fronts on the top of the jet tubes. Flame conditions and corresponding hot gas temperatures are presented in Table 1. The temperatures were measured at 5 mm above the burner outlet through two-line atomic fluorescence (TLAF) thermometry using indium atoms. The details of the technique were reported by Borggren et al. [19]. The uncertainty of the measured temperature was ~3%. A stabilizer was placed 35 mm above the burner outlet. Gas flows were controlled separately using mass flow controllers (Bronkhorst High-Tech) with an accuracy of ±0.8% of the reading value plus ±0.2% of the full-scale value.

$K_2CO_3$ and KCl water solution at 0.5 mol/l and 1.0 mol/l, respectively, were used as the potassium source in the hot flue gas. The water solution was atomized using an ultrasonic fog generator, and the fog was introduced to the jet chamber by an air flow of 0.5 l/min. Together with the premixed $CH_4/air/O_2$, $K_2CO_3$ and KCl water solution droplets were transported to the outlets of the jets and formed gas-phase KOH and KCl downstream of the hot flames. $SO_2$, used as the source of sulfur, was seeded through the co-flow chamber, which avoided any heterogeneous reactions between potassium and sulfur before they were introduced into the hot gas environment.

The concentrations of KOH, KCl, and OH were measured using UV absorption spectroscopy. The details of the measurements have been reported by Weng et al.[17]. In the measurements, a collimated UV beam with a diameter of ~10 mm generated by a deuterium lamp passed though the hot flue gas products at 5 mm above the burner outlet. The optical path length was extended by sending the beam through the hot gas five times using UV-enhanced aluminium mirrors. The light was collected and analysed using a spectrometer (USB 2000+, Ocean Optics). The concentrations of KOH, KCl, and OH were evaluated using the Beer-Lambert law. Typical absorbances are shown in Fig. 2, as 50 ppm $SO_2$ and 20 ppm KOH was seeded into the hot flue gas of flame T3O1. It can be seen that the

Table 1
Summary of the flame conditions, where the temperatures were measured 5 mm above the burner outlet.

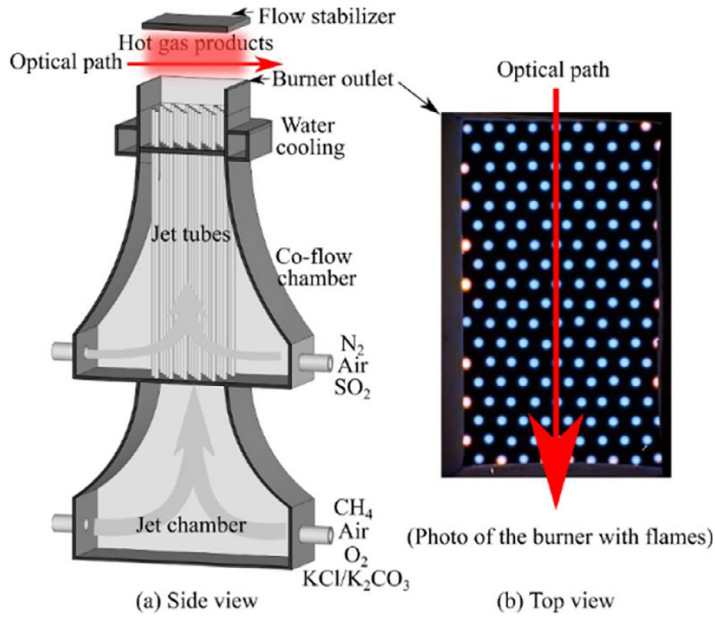| Flame Case | Gas flow rate (sl/min) | | | | | Fuel-oxygen equivalence ratio $\phi$ | Gas product temperature (K) |
|---|---|---|---|---|---|---|---|
| | Jet-flow | | | Co-flow | | | |
| | $CH_4$ | Air | $O_2$ | $N_2$ | Air | | |
| T1O1 | 2.47 | 12.23 | 2.58 | 18.97 | 8.90 | 0.70 | 1550 |
| T2O1 | 2.28 | 11.89 | 2.26 | 22.69 | 9.83 | 0.67 | 1390 |
| T3O1 | 2.09 | 10.90 | 2.07 | 26.50 | 10.66 | 0.63 | 1260 |
| T4O1 | 1.71 | 8.91 | 1.69 | 26.92 | 10.25 | 0.60 | 1120 |
| T4O2 | 2.28 | 7.82 | 1.84 | 27.90 | 0.00 | 1.31 | 1140 |



Fig. 1. (a) schematic of the multi-jet burner; (b) a photo of the burner with premixed flames anchored on the outlets of jet tubes.
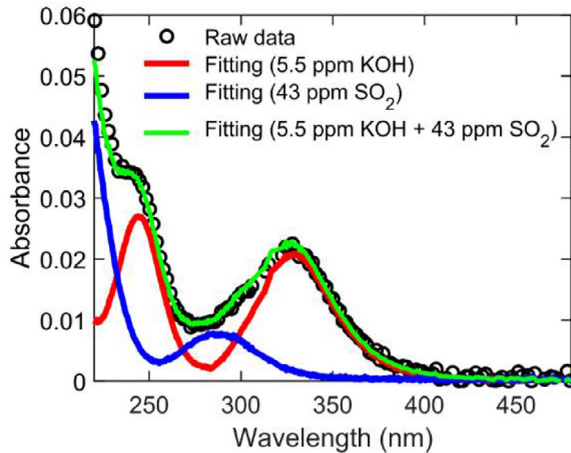


Fig. 2. The absorbance of KOH/SO$_2$ in the hot flue gas (T3O1, $\phi = 0.63$, $T = 1260$ K) with 20 ppm KOH and 50 ppm SO$_2$ seeding and the best fitting was given with 5.5 ppm KOH and 43 ppm SO$_2$.

absorption spectrum including both KOH and $SO_2$ can be fitted with the reported absorption cross sections of KOH [16] and $SO_2$ [20] with a concentration of 5.5 ppm and 43 ppm, respectively. The systematic error of the measurements mainly included the uncertainty of the UV absorption cross section of KOH and KCl, which is about 5% [16]. The standard deviation was derived from the measured absorbance. The concentration of the OH radical was derived as the absorbance at around 310 nm, fitted by the absorption cross section extracted from LIFBASE [17,21]. Since both KOH and $SO_2$ have broadband absorption and smooth absorption spectra was obtained at the high temperature, the narrowband absorption by OH radical can be easily extracted with a smooth baseline. The uncertainty of the OH concentration was originated from the absorbance curve-fitting process.

The concentration of atomic K was measured by TDLAS at 769.9 nm and 404.4 nm. The details of the potassium measurements have been reported by Weng et al. [16]. The system at 769.9 nm was used to measure K below hundreds ppb, while the one at 404.4 nm was adopted in measurements of K atoms at higher concentration. The uncertainty of the measured K atoms concentration includes the standard deviation of the measured absorbance and absorbance curve-fitting to the line shape function, giving a value of around ~5%.

Meanwhile, the 532 nm laser beam from a pulsed Nd:YAG laser (Quanta Ray) was used to illuminate the nucleated aerosols in the hot flue gas. The laser was formed into a laser sheet and guided through the hot gas region vertically. The resulting signal from aerosols was collected by a single-lens reflex camera (Canon, EOS2000D).

## 3. Model

The simulation of the sulfation process in the hot flue gas was conducted using Chemkin Pro [22]. In the simulation, the reaction mechanism developed by Weng et al. [13] (Supplementary Material 2) was adopted. The detailed modelling of the flows were described by Weng et al. [17]. A one-dimensional stagnation reactor model was used to simulate the reactions along the central axial of the burner. The mixture of the post-flame gases from 3 mm downstream of the premixed flames and the co-flow was used as the inlet gas of the stagnation reactor model. The post-flame gas composition was calculated using a one-dimensional free propagation premixed flame model. The concentrations of KOH and KCl were set to be the ones measured in the experiment without $SO_2$ seeding. The axial distance in the stagnation model was 6.4 cm, taken to be the distance between the outlet of the jets and the flow stabilizer. The temperature along the axial was assigned to be the one measured in the experiment using TLAF and a well-calibrated

B-type thermocouple (OMEGA). Along the lateral direction, a one-dimensional opposed-flow model in Chemkin-Pro was used to include the edge effect into the simulation results as reported by Weng. et al. [17]. The averaged concentration from the simulation along the horizontal direction at 5 mm above the burner outlet was used to compare with the experimental measurements. It should be noted that the processes at the very beginning of the mixing between the co-flow and the flue gas from premixed flames were not covered by the model. In the experiment, the mixing length could be 10-15 mm [9], while in the model, the inlet gas was taken to be fully mixed before reactions. This might cause some discrepancy between the experimental and simulation results.

## 4. Results and discussion

### 4.1. Sulfation in oxidative environment

Figure 3a presents the measured concentrations of KCl and K atom in the hot flue gas with around 20 ppm KCl and varying amounts (50–150 ppm) of $SO_2$ seeding. The hot flue gas at 1120 K was provided by flame T4O1 with a fuel-oxygen equivalence ratio of 0.6. At this temperature, almost no KCl was transformed to KOH. The concentrations of KCl and K atoms decreased with increasing $SO_2$ seeding. As 150 ppm $SO_2$ was introduced into the flame, the concentration of K atoms was reduced from 0.17 ppb to 0.07 ppb, and the concentration of KCl was decreased from 20 ppm to 14 ppm. The reduction of KCl and K atom was caused by the sulfation of potassium into gaseous $KHSO_4$ and $K_2SO_4$, and $K_2SO_4$ aerosols, as reported by Li et al. [9]. The model predicted well the concentration of K atom, while the sulfation of KCl was overpredicted (cf. Fig. 3a). This might be due to the fact that at this temperature, the sulfation of KCl was controlled by the concentration of $SO_2$ [12,13]. In the model, the assumption of full mixing between KCl and $SO_2$ at the very beginning made the sulfation of KCl more rapid than observed. In the simulation, gaseous $KHSO_4$ and $K_2SO_4$ were predicted to be the main products of the sulfation of KCl, and they were at similar concentration levels (cf. Fig. 3a). The major sulfation pathway was predicted to occur through the reactions among K, $O_2$ and $SO_2$ in forming $KHSO_4$ and $K_2SO_4$ through $KOSO_3$ [13] at this temperature. Atomic K, formed from $KCl+H=K+HCl$ (R1), form $KOSO_3$, either through $K+O_2(+M)=KO_2(+M)$ (R2), $KO_2+SO_2(+M)=KOSO_3(+M)$ (R3), or via $K+SO_2(+M)=KOSO(+M)$ (R4), $KOSO+O_2(+M)=KOSO_3(+M)$ (R5). $KOSO_3$ is then rapidly converted to sulfate through the sequence $KOSO_3+H_2O=KHSO_4+OH$ (R6), $KHSO_4+KCl=K_2SO_4+HCl$ (R7), $KOSO_3+KCl=K_2SO_4+Cl$ (R8).
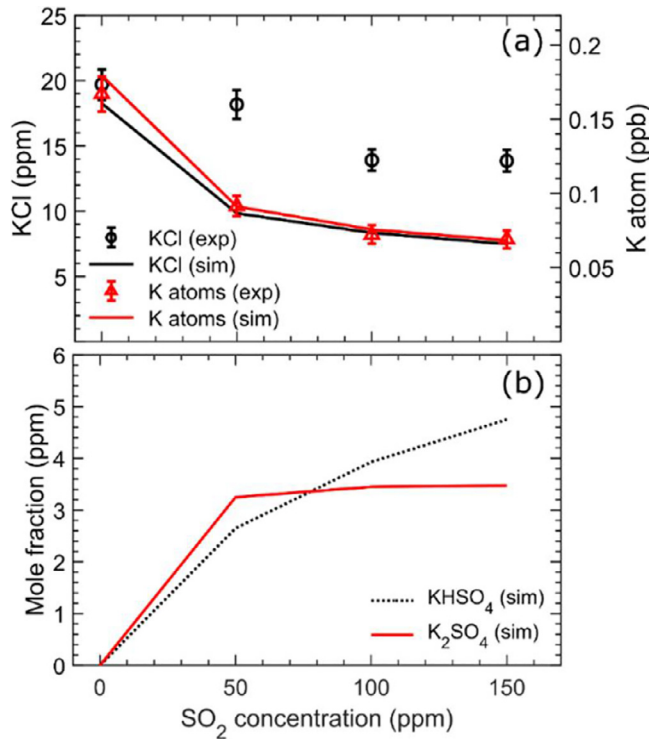
Fig. 3. Concentration of KCl and K atoms from both experimental measurement and modelling prediction (a) and the predicted concentration of $KHSO_4$ and $K_2SO_4$ (b) versus the amount of $SO_2$ in the hot flue gas T4O1 ($\phi = 0.6$, $T = 1120$ K) with 20 ppm KCl seeding.

To characterize the sulfation of KOH in the hot gas environments, $SO_2$ was introduced into the hot flue gas containing ∼20 ppm KOH. The KOH was generated through the seeding of $K_2CO_3$, which rapidly reacts with water vapour to form KOH and eventually K atoms as it passes through the hot flame zone. Similar to the sulfation of KCl, the presence of $SO_2$ lead to reduced concentrations of KOH and K atoms, especially at the low temperature cases, as shown in Fig. 4. Both KOH and K atom were almost fully removed as above 50 ppm $SO_2$ was seeded, and the sulfation of KOH was apparently more effective than KCl. The consumed KOH was transformed partly into condensed $K_2SO_4$ aerosols observed as the strong Mie scattering in the hot flue gas with a temperature lower than 1260 K (cf Figs. 4e and f) at which the vapour pressure of $K_2SO_4$ is lower than 0.002 mbar [7]. The sulfation process was weakened in higher temperature, where more KOH and K survived (Figs. 4a and 4b) and less aerosols were generated (Figs. 4c–f). As the temperature reached 1390 K and 1550 K, the $SO_2$ seeding had almost no influence on the concentration of K atom, and no aerosols were observed, while still a certain amount of KOH was consumed. This indicated that gaseous potassium–sulfur compounds were generated in the sulfation

process, mostly gaseous $KHSO_4$ and $K_2SO_4$ according to the model. The modelling results, as presented in Figs. 4a and 4b, captured well the varying trend of the concentration of KOH and K atom as function of the amount of $SO_2$ seeding. Especially for the KOH concentration, under most conditions, the simulation and experimental results were in good agreement, in contrast to the cases for KCl. As reported by Weng et al. [13], the sulfation of KOH at this temperature was no longer relying on the existence of high $SO_2$ concentration and the partial mixing between KOH and $SO_2$ at the very beginning had no influence on the whole sulfation process. The sulfation pathway of KOH was similar to that of KCl as presented above, but the results showed a higher propensity for sulfation of KOH. We attribute this to the lower thermal stability of KOH, which resulted in the formation of higher levels of K atoms. The sulfation of KOH was strongly dependent on the temperature. During the mixing of the cold co-flow and the hot post-flame gas close to the jets, there might exist low temperature zones which was not included in the modelling. This low temperature zone would promote KOH sulfation, such as for the case at 1390 K shown in Fig. 4a, where the model underpredicted the sulfation of KOH. The
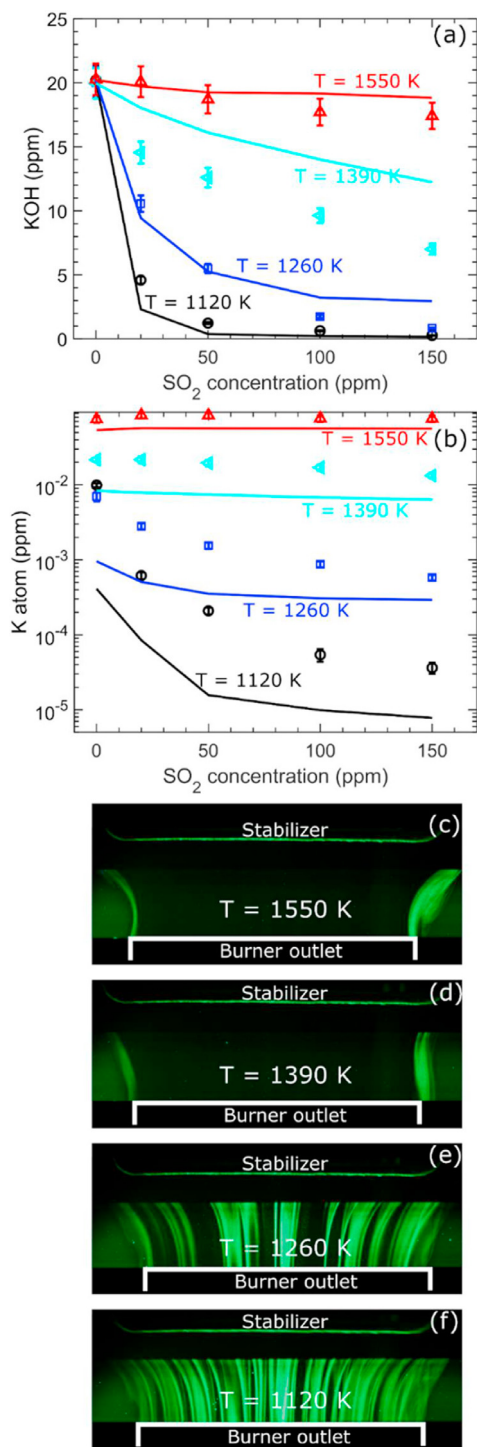
Fig. 4. Concentration of KOH (a) and K atom (b) versus the amount of $SO_2$ in the hot flue gas from the flame T1O1-T4O1 with 20 ppm KOH seeding, and the scattering of aerosols in the hot flue gas from the flame T1O1-T4O1 with 20 ppm KOH and 150 ppm $SO_2$ seeding (c-f).
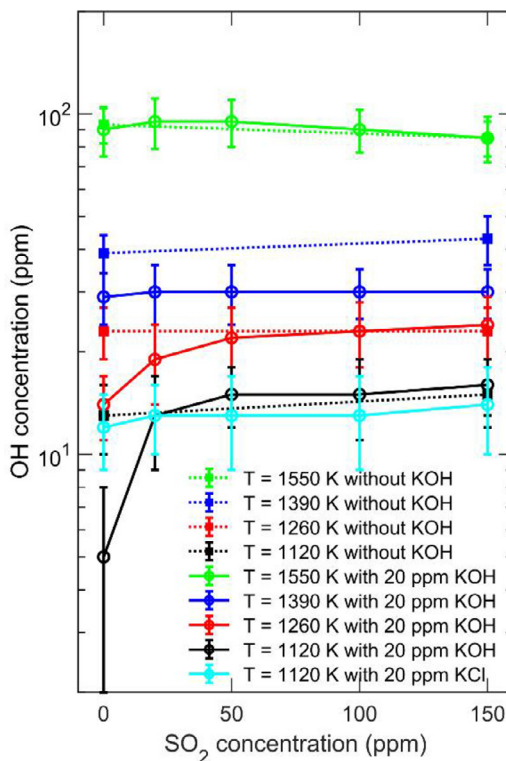


Fig. 5. Concentration of OH radicals versus the amount of $SO_2$ in the hot flue gas from different flames with or without 20 ppm KCl or KOH seeding.

predicted sulfation reactions, besides the ones presented above for KCl, include $KOH+H=K+H_2O$ (R9), $KHSO_4+KOH=K_2SO_4+H_2O$ (R10), and $KOSO_3+KOH=K_2SO_4+OH$ (R11).

The concentration of the OH radical in the hot flue gas is shown in Fig. 5. In the absence of $SO_2$ at 1120 K, the addition of KOH lead to a significant reduction of OH, while the KCl seeding had almost no effect. The effect of KOH was mainly attributed to the chain terminating reaction sequence $KOH+H=K+H_2O$ (R9), $K+OH+M=KOH+M$ (R12). As $SO_2$ was added into the hot flue gas, KOH was sulphated, eliminating the terminating sequence. With only $SO_2$ seeding, there is no change in the OH radical concentration. For the cases having relatively low temperatures, i.e., 1120 K, 1260 K and 1390 K, the KOH seeding promoted OH radical consumption. The sulfation by $SO_2$ seeding reduced the concentration of K atom significantly at the temperatures of 1120 K and 1260 K (cf. Fig. 4b), resulting in the OH concentration not being affected by the KOH seeding. However, at 1390 K, the concentration of K atom did not decrease due to sulfation and consequently the KOH seeding did not reduce the OH concentration.

### 4.2. Sulfation in reducing environments

The sulfation process of potassium hydroxide in a reducing hot environment was investigated using the flame T4O2 with a global equivalence ratio of 1.31 and a temperature 1140 K. The concentration of potassium introduced into the hot gas was 22 ppm. In the reducing environment without $SO_2$ seeding, 14 ppm K atoms were formed, which contributed significant absorption at 404 nm (cf. Fig. 6a), accompanied by 8.5 ppm KOH. When $SO_2$ was seeded into the hot flue gas, the concentration of K atom decreased dramatically. Some extra structures in the UV absorption spectra distinguished from KOH and $SO_2$ were observed in the hot flue gas with both KOH and $SO_2$ seeding, especially at wavelengths above 350 nm, as shown in Fig. 6a. To the authors' knowledge, this absorption profile has not been reported in any previous related work. According to predictions for the K-S chemistry in a reducing environment, KOSO becomes the dominant species at temperatures around 1000 K [13]; in the absence of $O_2$, KOSO cannot be oxidized to $KOSO_3$ through R5. Hence, the unknown absorption spectrum was attributed to KOSO. In order to identify the KOSO absorption spectrum, the absorbance of the specific amounts of KOH and $SO_2$ remaining after sulfation was subtracted from the absorbance obtained from the hot flue gas. After subtraction, the absorbance spectra were normalized. The amount of remaining KOH and $SO_2$ were adjusted to make sure that the normalized absorbance had the identical structure, as shown in Fig. 6b. Through this, the concentration of the remaining KOH was obtained, and the concentration of KOSO was evaluated through the subtraction of the K and KOH from the total potassium, i.e., 22 ppm. The remaining absorbances attributed to KOSO from the cases with different amount $SO_2$ seeding are presented in Fig. 6c as a function of the corresponding KOSO concentration. A good linear relationship was obtained. Using this relationship, the absorption cross sections of KOSO was derived based on the Beer-Lambert law, and corresponding values are presented in Fig. 6d.

The concentrations of KOH, K atom and the rest attributed to KOSO, as functions of the amount of $SO_2$ seeding are shown in Fig. 7. The KOSO yield increased with the $SO_2$ concentration, and as 150 ppm $SO_2$ was seeded into the reducing hot environment, almost all of the 22 ppm potassium was converted to KOSO. The model predicted correctly the trend of K atom decrease and the KOSO increase with $SO_2$ seeding, but overpredict the K atom and under-predict the KOH concentrations compared to the experimental results.

In the absence of $SO_2$, the model predicted that potassium is largely present as K atom; this is in
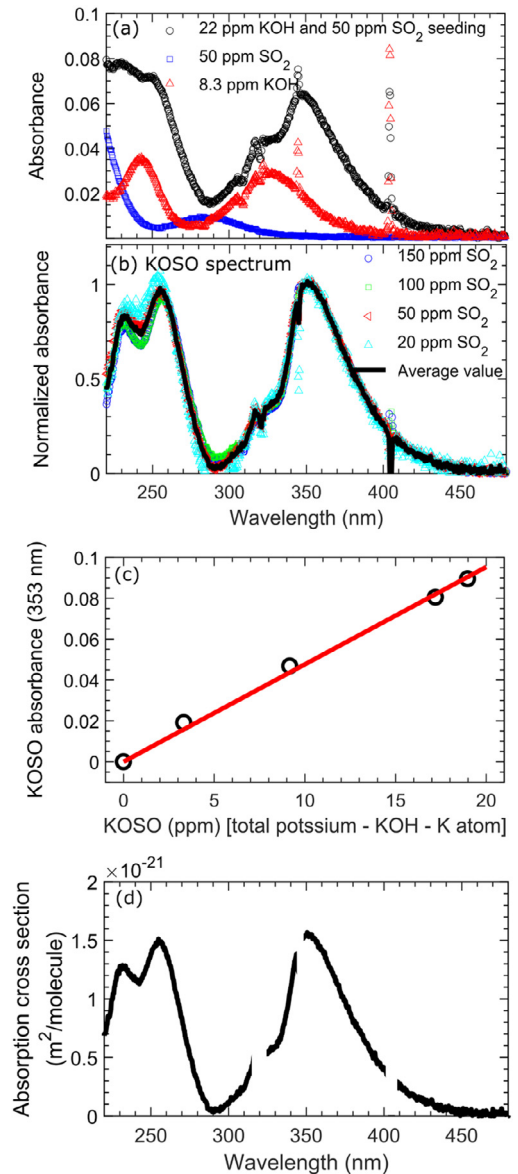


Fig. 6. (a) Spectral curves of the absorbance when 8.3 ppm KOH (red), or 50 ppm $SO_2$ (blue), or simultaneously with 50 ppm $SO_2$ and 22 ppm KOH (black) seeded into flame T4O2 ($T = 1140$ K and $\phi = 1.31$); (b) normalized absorbance of KOSO under different conditions with varying amount of $SO_2$ seeding (from 20 ppm to 150 ppm); (c) the absorbance of KOSO at 353 nm versus its concentration, which was obtained through the subtraction of total 22 ppm KOH by the concentration of KOH and K atom; (d) the estimated UV absorption cross section of KOSO.
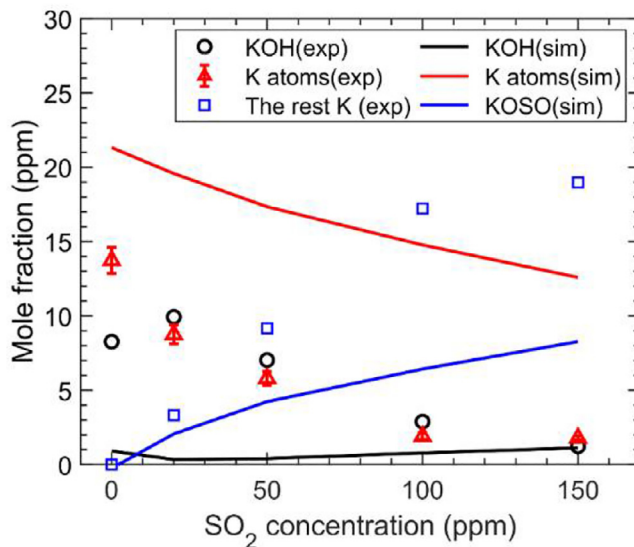
Fig. 7. Concentration of KOH, K atoms and the rest K assumed to be KOSO versus the amount of $SO_2$ in the hot flue gas T4O2 ($\phi = 1.31$, $T = 1140$ K) from experimental measurement and simulation.

contrast to the measurements, which showed significant amounts of KOH. The cause of this behaviour, which was also reported by Weng et al. [17], is not clear at present. At the high temperatures in the flame region, KOH is fully converted to K atom. Above the flame, as the temperature decreases, the formation of KOH is favoured. However, due to the low levels of radicals at the lower temperatures, the $K+OH$ recombination reaction is slow. The underprediction of KOH could indicate missing pathways in the reaction mechanism, significant under reducing conditions.

When is $SO_2$ added, atomic K is converted to KOSO through the reaction R4, $K+SO_2(+M)=KOSO(+M)$. Under the conditions shown in Fig. 7, this reaction is close to partial equilibrium, according to the model. This indicates that the underprediction of KOSO by the model could be caused by uncertainties in the thermodynamic properties of KOSO. The heat of formation of KOSO in the model is based on bond strength of $K-SO_2$ of $190 \pm 11$ kJ/mol, as determined by Goumri et al. [23]. The present experimental results indicate that the bond strength of $K-SO_2$ may be larger than this value, but more work is needed to confirm this.

## 5. Conclusion

Optical in situ measurements were performed for the quantitative investigation of K-Cl-S gasphase chemistry in a well-defined high-temperature atmosphere. Both oxidative and reducing environments were investigated with temperature varying from 1120 K to 1550 K. The concentrations of KOH, KCl and OH in the hot gas were measured by UV absorption spectroscopy, and the concentration of K atoms was obtained using TDLAS systems at 769.9 nm and 404.4 nm. A higher propensity for sulfation was observed at lower temperatures, and sulfation of KOH was more rapidly compared to KCl. In the sulfation of KOH, aerosols were observed and the concentration of K atoms was significantly reduced at temperatures of 1120 K and 1260 K. At 1390 K, KOH was consumed with $SO_2$ seeding, but no aerosols were observed. K atoms generated from KOH enhanced the consumption of OH radicals, and the concentration of OH in the hot flue gas was strongly related to the concentration of K atoms. The sulfation by adding $SO_2$ reduced the K atom concentration significantly at low temperatures, causing less consumption of OH radicals. Also, in a reducing atmosphere at 1140 K, the presence of $SO_2$ leads to the consumption of K atom and KOH. A UV absorption spectrum, distinguished from those of KOH and $SO_2$, was obtained; it was attributed to KOSO. The detailed K-Cl-S chemical mechanism reported by Weng et al. [13] was evaluated, and reasonable agreement between the simulation and experimental results was obtained. The knowledge of the sulfation of KOH/KCl and the formation of $K_2SO_4$ aerosols supports the improvement of design and operation of biomass gasifiers with less slagging and corrosion, and controlled particle emission.

## Declaration of Competing Interest

## Acknowledgments

## Supplementary materials

Supplementary material associated with this article can be found, in the online version, at doi:10.1016/j.proci.2020.05.058.

## References

[1] K. Iisa, Y. Lu, K. Salmenoja, *Energy Fuels* 13 (1999) 1184–1190.
[2] P. Glarborg, P. Marshall, *Combust. Flame* 141 (2005) 22–39.
[3] S. Jiménez, J. Ballester, *Combust. Flame* 140 (2005) 346–358.
[4] M. Aho, P. Vainikka, R. Taipale, P. Yrjas, *Fuel* 87 (2008) 647–654.
[5] L. Hindiyarti, F. Frandsen, H. Livbjerg, P. Glarborg, P. Marshall, *Fuel* 87 (2008) 1591–1600.
[6] H. Kassman, L. Bäfver, L.-.E. Åmand, *Combust. Flame* 157 (2010) 1649–1657.
[7] M.U. Garba, D.B. Ingham, L. Ma, et al., *Energy Fuels* 26 (2012) 6501–6508.
[8] H. Kassman, F. Normann, L.-.E. Åmand, *Combust. Flame* 160 (2013) 2231–2241.
[9] B. Li, Z. Sun, Z. Li, et al., *Combust. Flame* 160 (2013) 959–969.
[10] T. Ekvall, F. Normann, K. Andersson, F. Johnsson, *Energy Fuels* 28 (2014) 3486–3494.
[11] H. Wu, M.N. Pedersen, J.B. Jespersen, et al., *Energy Fuels* 28 (2014) 199–207.
[12] T. Ekvall, K. Andersson, T. Leffler, M. Berg, *Proc. Combust. Inst.* 36 (2017) 4011–4018.
[13] W. Weng, S. Chen, H. Wu, P. Glarborg, Z. Li, *Fuel* 224 (2018) 461–468.
[14] M.R. Mortensen, H. Hashemi, H. Wu, P. Glarborg, *Fuel* 258 (2019) 116147.
[15] Y.A. Situmorang, Z. Zhao, A. Yoshida, A. Abudula, G. Guan, *Renew. Sustain. Energy Rev.* 117 (2020) 109486.
[16] W. Weng, C. Brackmann, T. Leffler, M. Aldén, Z. Li, *Anal. Chem.* 91 (2019) 4719–4726.
[17] W. Weng, Y. Zhang, H. Wu, P. Glarborg, Z. Li, *Fuel* 271 (2020) 117643.
[18] W. Weng, J. Borggren, B. Li, M. Aldén, Z. Li, *Rev. Sci. Instrum.* 88 (2017) 045104.
[19] J. Borggren, W. Weng, A. Hosseinnia, P.-.E. Bengtsson, M. Aldén, Z. Li, *Appl. Phys. B* 123 (2017) 278.
[20] W. Weng, M. Aldén, Z. Li, *Anal. Chem* 91 (2019) 10849–10855.
[21] LIEBASE, version 2.1. https://www.sri.com/contact/form/lifbase.
[22] Reaction Design, CHEMKIN-PRO 15131 San Diego, 2013.
[23] A. Goumri, D. Laakso, J.D.R. Rocha, E. Francis, P. Marshall, *J. Phys. Chem.* 97 (1993) 5295–5297.